Environmental Advances 9 (2022) 100296

Contents lists available at ScienceDirect

Environmental Advances

journal homepage: www.sciencedirect.com/journal/environmental-advances

A review of new TDR applications for measuring non-aqueous phase liquids (NAPLs) in soils

Alessandro Comegna [a,*], Gerardo Severino [b], Antonio Coppola [a]

[a] School of Agricultural Forestry Food and Environmental Sciences (SAFE), University of Basilicata, Potenza, Italy
[b] Department of Agriculture, University of Naples "Federico II", Italy

ARTICLE INFO

Keywords:
Time domain reflectometry technique
Soil contamination
Soil-NAPL-water mixtures
Dielectric properties
Mixing models

ABSTRACT

The time domain reflectometry (TDR) technique is a geophysical method that allows, in a time-varying electric field, the determination of dielectric permittivity and electrical conductivity of a wide class of porous materials. Measurements of the volumetric water content (θ_w) in soils is the most frequent application of TDR in Soil Science and Soil Hydrology. In last four decades several studies have sought to explore potential applications of TDR. Such studies (except those conducted on θ_w estimation) mainly focused on monitoring soil solute transport. In more recent times, innovative TDR approaches have also been implemented to extend current TDR fields of application to the problem of monitoring non-aqueous phase liquids (NAPLs) in variable saturated soils. NAPLs are organic compounds with low solubility in water and are characterised by a high mobility in the vadose zone. Due to their high toxicity, NAPLs constitute a severe geo-environmental problem, thus making detection and observation of such substances in soils an increasingly important issue. The present paper deals with these studies and aims to provide an up-to-date review of the main NAPL-TDR studies. To date, the literature has focused on TDR applications in three main fields: (i) NAPL monitoring in homogeneous, variable saturated soils, (ii) NAPL monitoring in layered variable saturated soils, and (iii) NAPL monitoring during soil decontamination processes. For an exhaustive and complete overview of TDR research in this field, we also recall the basic principles of TDR signal propagation, the functioning of a typical TDR device, and the dielectric mixing models that are widely used to interpret the dielectric response of NAPL-contaminated soils.

1. Introduction

In the last four decades, the TDR technique has represented the most widely used method to estimate bulk dielectric permittivity (ε_b) and bulk electrical conductivity (EC_b) in soils, as well as in other porous materials (Topp et al., 1980; Topp et al., 1982; Dalton et al., 1984; Topp and Davis, 1985; Rhoades et al., 1989; Persson, 1997; Hilhorst, 2000; Jones et al., 2002; Huisman et al., 2008; Comegna et al., 2013c; Coppola et al., 2012; Coppola et al., 2015; Dragonetti et al., 2018; Comegna et al., 2022 among others). Based on this feature, TDR has been widely used to monitor contaminant distribution and transport in soils (see e.g., Jones et al., 2002; Huisman et al., 2008; Coppola et al., 2011a; Comegna et al., 2020), which is of crucial interest in such fields as agriculture and environmental sciences.

On this topic, many experiments were carried out using different tracers such as bromide (Wraith et al., 1993; Persson and Berndtsson, 1998; Carpena et al., 2005), chloride (Kachanoski et al., 1992; Vanclooster et al., 1993; Mallants et al., 1994; Vanclooster et al., 1995; Vogeler et al., 1996; Vogeler et al., 1997; Comegna V. et al., 1999; Vanderborght et al., 2000; Vanderborght et al., 2001; Comegna V. et al., 2001; Comegna et al., 2003; Noborio et al., 2006; Coppola et al., 2009; Severino et al., 2010; Coppola et al., 2011b; Coppola et al., 2015; among others), nitrate (Payero et al., 2006; Comegna V. et al., 2011; Miyamoto et al., 2015), heavy metals and pesticides (Mojid et al., 2016).

In recent years, in addition to the above applications, new TDR-based approaches were developed to extend TDR fields of application to the issue of monitoring NAPL dynamics in variable saturated soils.

NAPLs are organic compounds with low or no solubility in water. They are substances which mainly belong to the family of petroleum products that may be accidentally introduced into the soil system. Extensive production and use of these products have provided abundant opportunities for soil and groundwater contamination (mainly due to the diffuse presence of abandoned industrial sites, poor disposal practices, accidental spills from petrol stations, oil fields, refineries, and so

* Corresponding author.
E-mail address: alessandro.comegna@unibas.it (A. Comegna).

https://doi.org/10.1016/j.envadv.2022.100296
Received 4 August 2022; Received in revised form 13 September 2022; Accepted 26 September 2022
Available online 27 September 2022

forth).

NAPLs exist in a separate phase in soils. This aspect increases the complexity of the subsurface system and difficulties in detection. Furthermore, due to their toxicity (even at low concentrations of a few parts per billion) and mobility, NAPLs may pose an increasing environmental threat to natural resources such as soil and water.

This has led several scientists to develop new strategies and methodologies to detect such pollutants.

Typically, NAPL monitoring in soils is performed by using invasive techniques that are based on soil drilling, sampling, and the installation of monitoring wells for the collection of soil and water samples (Mercer and Cohen, 1990). However, such approaches are costly, time-consuming and difficult to automate to collect real-time data.

To overcome such difficulties and limitations, geophysical methods (e.g., radar, resistivity and conductivity) may represent an alternative choice (Redman et al., 1991). In particular, a fair number of studies have shown the potential of the TDR technique to monitor NAPLs in saturated and unsaturated soils (see, for example, Persson and Berndtsson, 2002; Haridy et al., 2004; Mohamed and Said, 2005; Moroizumi and Sasaki, 2008; Rinaldi and Francisca, 2006; Francisca and Montoro, 2012; Comegna et al., 2013b; Zhan et al., 2013; Zhan et al., 2014; Comegna et al., 2016; Comegna et al., 2017). Most of such studies have demonstrated that the TDR method offers the possibility to quantitatively discriminate between NAPL and water in the TDR sampling volume (Persson and Berndtsson, 2002). This is made possible using new algorithms that work, for example, on analyzing the TDR signal amplitude at relatively long times from the waveform source (i.e., when multiple reflections have died out; Comegna et al., 2016). Other approaches are based on dielectric mixing models that, once calibrated and validated, permit the TDR dielectric response to be linked directly to the volumetric NAPL content θ_{NAPL} (Francisca and Montoro 2012; Comegna et al., 2016; Comegna et al., 2020). In other studies, measurements of ε_b and EC_b are collected and used together to discriminate NAPL presence in soils (Haridy et al., 2004; Zhan et al., 2013; Comegna et al., 2017).

After shortly recalling the main theoretical basis to be applied for NAPL monitoring by TDR, the paper will provide details on NAPL studies that have been conducted, at a laboratory scale, on a series of soils of different textures and structures.

2. Theoretical principles of TDR signal propagation in a finite transmission line embedded into homogeneous and layered media

In this section, we provide details on TDR signal propagation, mainly concerning NAPL monitoring approaches based on TDR. The basic TDR unit consists of: (i) a pulse or step generator, which produces a fast rise-time step voltage pulse; (ii) a sampler which transforms a high-frequency signal into a lower frequency output, and (iii) an oscilloscope. A synoptic diagram of the device is shown in Fig. 1a. The step generator produces an EM signal that travels along the coaxial line with an initial voltage of amplitude V_0. The transmission line has a nominal impedance Z_0=50 Ω until the signal reaches point A, where the voltage step V_0 is detected and displayed on the oscilloscope (Fig. 1b). The signal is now introduced into the coaxial line connecting the probe equipment: point B (cable-probe interface) represents a change in impedance (Z_{PROBE}) at the base of the probe. Once the transient signal reaches a discontinuity (i.e., a change in impedance) in the propagation line, part of the signal will be reflected to the generator, and will be added in-phase, or out-of-phase, to a new incident signal (Mohamed, 2006). Thus, at interface B, a portion of the signal (V_r) is reflected to the source, while the remaining fraction (V_t) is transmitted within the probe until it arrives at point C.

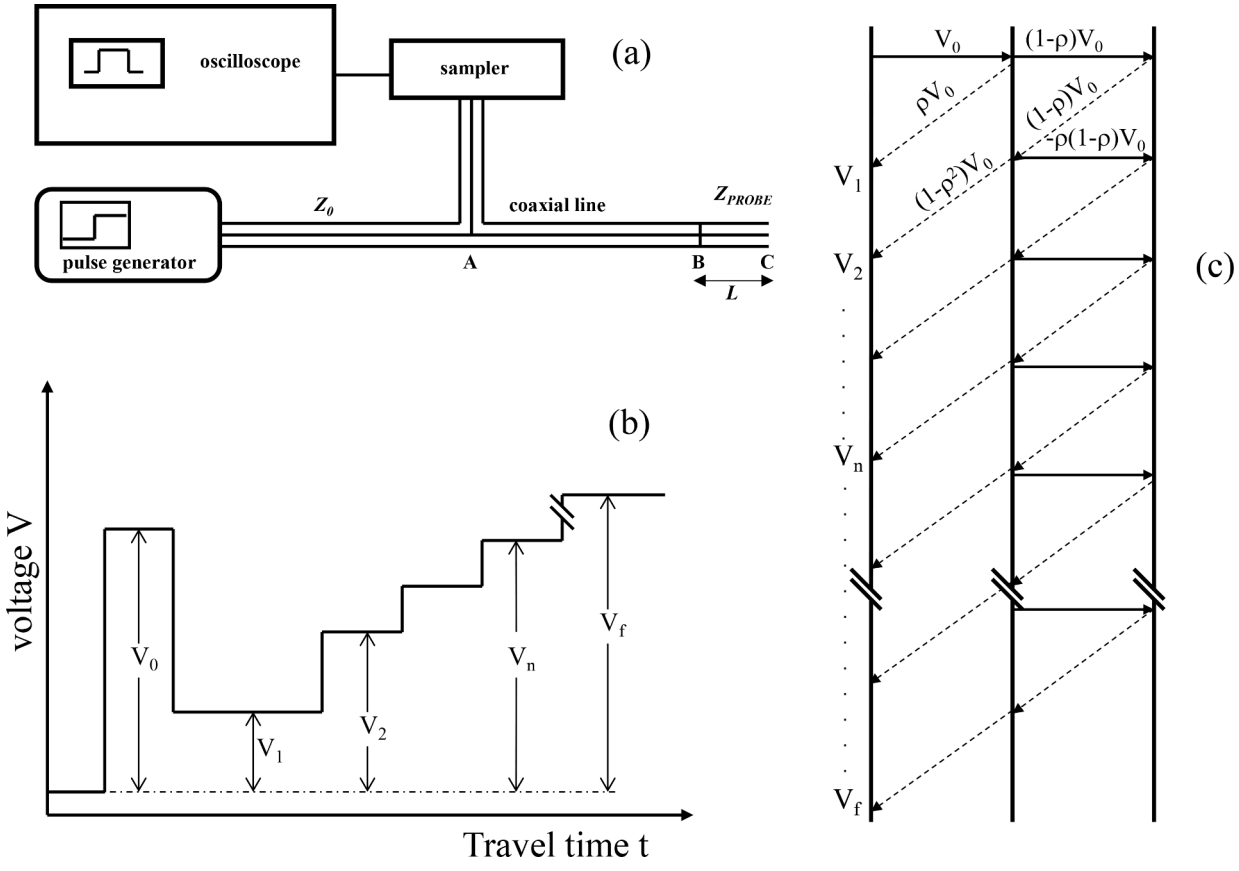

Fig. 1. (a) Time domain reflectometry (TDR) hardware setup, (b) voltage versus travel time for an idealized TDR waveform, and identification of distinctive signal characteristic, and (c) pattern of multiple reflections from a transmission line.

The magnitude of the reflection can be quantified through the reflection coefficient (i.e., the ratio of reflected to incident wave; Giese and Tiemann, 1975; Krauss, 1984) as a function of the impedance:

$$\rho = \frac{Z_{PROBE} - Z_0}{Z_{PROBE} + Z_0} \tag{1}$$

or as a function of the voltage:

$$\rho = \frac{V_i - V_0}{V_0} \tag{2}$$

where V_i is the amplitude of the reflected signal at a certain transit time t_i.

The range of values for ρ is between -1 (the EM is delivered back through the ground) and 1 (the EM is completely reflected to the source, Noborio, 2001). At point B, the reflected signal $V_r(=\rho V_0)$ is added to the incident signal (V_0), producing an additional signal of amplitude (Topp et al., 1988):

$$V_1 = V_0 + V_r = V_0 + \rho V_0 = (1+\rho)V_0 \tag{3}$$

The remainder of the wave not reflected at point B travels with an amplitude $V_t = (1-\rho)V_0$ to point C, where the EM is completely reflected in-phase, along the waveguides, because the end of the probe serves as an open-end circuit with infinite impedance (Topp et al., 1980; Mohamed, 2006; Lin et al., 2007, 2015). Part of the returning signal, when it reaches the cable/probe interface, is once again reflected downward (till point C), and part of it of magnitude $(1-\rho^2)V_0$ arrives at the TDR Unit, which records the voltage:

$$V_2 = V_1 + \left(1-\rho^2\right)V_0 = (1+\rho)V_0 + \left(1-\rho^2\right)V_0 \tag{4}$$

A complex pattern of gradually decreasing reflections is thus generated (Fig. 1c). The step amplitude of the nth-order reflection is as follows (Yanuka et al., 1988; Feng et al., 1999):

$$V_n = V_0\left[(1+\rho) + \left(1-\rho^2\right)\sum_{k=0}^{n-2}(-\rho)^k\right] \tag{5}$$

where k denotes the number of reflections converging at the air-soil interface (in a homogeneous medium k=3). Eq. (5) is valid for a number of reflections $n \geq 2$ and for a non-conductive medium. In an attenuating medium, Yanuka et al. (1988) suggest that the magnitude of the signal decreases by an attenuation factor:

$$f = \exp(-2L\alpha) \tag{6}$$

where α is the attenuation coefficient (which mainly depends on the conductive and dielectric properties of the medium), and L is the probe length. In this case, Eq. (5) can then be written as:

$$V_n = V_0\left[(1+\rho) + \left(1-\rho^2\right)\sum_{k=0}^{n-2}(-\rho)^k(f)^{k+1}\right] \tag{7}$$

The asymptotic voltage value V_f (i.e., the measured voltage at long travel times) is:

$$V_f = V_0\left[(1+\rho) + \frac{f^2(1-\rho^2)}{1+\rho f^2}\right] \tag{8}$$

3. Dielectric measurements using TDR

It is generally recognized that the dielectric permittivity of liquids and solids can be described by a complex number ε^* (Robinson and Friedman, 2002). At the highest TDR working frequencies (i.e., from 200 MHz to 1.5 GHz), where dielectric losses can be assumed to be negligible, ε^* reduces to the real part only ε' (Heimovaara, 1994). Using a waveguide (or probe) of known length L, ε' ($\cong$ the bulk dielectric permittivity ε_b) is measured from the propagation velocity $v(=2L/t)$ of an electromagnetic wave along the waveguide through the soil by:

$$\varepsilon' = \varepsilon_b = \left(\frac{c}{v}\right)^2 \tag{9}$$

where c ($=3*10^8$ m s^{-1}) is the velocity of an EM wave in the vacuum, t (s) is the travel time, that is the time that the EM pulse needs to traverse back and forth along the TDR-rods of length L (m), and can be written as:

$$t = \frac{2L}{c}\sqrt{\varepsilon_b} \tag{10}$$

which yields the direct dependence between the travel time t of the signal and ε_b.

Another fundamental dielectric property that can be obtained from a TDR signal is the bulk electrical conductivity, EC_b, related to the magnitude of energy attenuation, which can be calculated, for example, using the thin-section approach of Giese and Tiemann (1975):

$$EC_b = \frac{K_G}{Z_0}\left(\frac{2V_0}{V_f} - 1\right) \tag{11}$$

where K_G is the geometric constant of the probe of length L. This quantity needs to be estimated with a specific empirical procedure by immersing the TDR probe in various solutions of known electrical conductivity (Persson and Berndtsson, 2002).

Other equations relevant to estimating EC_b may be found in Dalton et al. (1984), Topp et al. (1988), Yanuka et al. (1988), Nadler et al. (1991), Lin et al. (2007) and (2008). All these methods provide a good evaluation of EC_b, especially in the range 0 to 2 dS/m.

4. Dielectric mixing models for NAPL estimation

Dielectric mixing models are a valid alternative to using empirically derived functions to characterize the dielectric behaviour of a medium (Dobson et al., 1985; Dirksen et al., 1993). The mixing laws link the bulk dielectric permittivity of a multi-phase medium to the dielectric response of each single phase (Hilhorst, 1998; Coppola et al., 2013; Regalado et al., 2003; Comegna et al., 2013a). In their classical application, these equations described the soil as a mixture of two (e.g.., soil-water), three (e.g., soil-water-air) or four (e.g., soil-free water--bound water-air) dielectric phases. The composite dielectric permittivity of the investigated medium depends on the relative weight of each single phase.

Among the many physical models of dielectric permittivity available in the literature (De Loor, 1964; Dobson et al., 1985; Regalado et al., 2003, among others), one of the most widely used mixing models is the so-called α-model (Birchak et al., 1974; Roth et al., 1990; Hilhorst, 1998):

$$\varepsilon_b^\alpha = \left[\sum_{i=1}^{n} W_i\varepsilon_i^\alpha\right] \tag{12}$$

where W_i and ε_i are the volume and the permittivity, respectively, of each component, and the exponent α is a curve-fitting parameter that is correlated with the internal structure of the medium (it ranges between -1 and 1). In particular, this geometric factor is related to the direction of the effective layering of the different dielectric components to the direction of the applied electrical field (Hilhorst, 1998).

For mixtures of soil saturated with water (sw), and for soil-water-air (swa) compounds, the α model can be written as:

$$\varepsilon_{sw}^\alpha = \left[(1-\phi)\varepsilon_s^\alpha + \phi S\varepsilon_w^\alpha\right] \tag{13}$$

$$\varepsilon_{swa}^\alpha = \left[(1-\phi)\varepsilon_s^\alpha + \phi S\varepsilon_w^\alpha + \phi(1-S)\varepsilon_a^\alpha\right] \tag{14}$$

where ε_{sw} and ε_{swa} are, respectively, the dielectric permittivities of the soil-water and soil-water-air mixtures, ε_s, ε_w, ε_a are the permittivities of

soil particles, water, and air, respectively, S is the effective water saturation and ϕ is the porosity of the sample.

Recently these models have been extended to estimate the bulk dielectric properties of NAPL-contaminated soils (Persson and Berndtsson, 2002; Francisca and Montoro, 2012; Comegna et al., 2013a; Comegna et al., 2016). In this case, following the approach of Rinaldi and Francisca (2006), the contaminated medium can be schematized, from a dielectric point of view, as a mixture of soil, air and NAPL (*saNAPL*), with soil, water and air:

$$\varepsilon_b^\alpha = \left[\beta\varepsilon_{saNAPL}^\alpha + (1-\beta)\varepsilon_{swa}^\alpha\right] \quad (15)$$

where β is the so-called relative volume of NAPL in water:

$$\beta = \frac{\theta_{\mathrm{NAPL}}}{(\theta_w + \theta_{\mathrm{NAPL}})} = \frac{\theta_{\mathrm{NAPL}}}{\theta_f} \quad (16)$$

$\theta_f(=\theta_w+\theta_{\mathrm{NAPL}})$ being the volumetric fluid content, the sum of the volumetric water content (θ_w) and the volumetric NAPL content (θ_{NAPL}); β ranges between 0 (i.e., soil-water mixtures) and 1 (i.e., soil-NAPL mixtures).

In Eq. (15), the term ε_{saNAPL} (which is the dielectric permittivity of the soil-air-NAPL mixture) can be written as:

$$\varepsilon_{saNAPL}^\alpha = \left[(1-\phi)\varepsilon_s^\alpha + \phi S\varepsilon_{NAPL}^\alpha + \phi(1-S)\varepsilon_a^\alpha\right] \quad (17)$$

where ε_{NAPL} is the dielectric permittivity of the NAPL.

5. TDR studies on NAPL monitoring in soils

TDR studies on NAPLs are grounded on the basic principle that their presence in soils affects the dielectric response of a contaminated medium. In general, in a partly saturated contaminated soil, for a constant θ_w, the measured ε_b of the medium decreases as NAPL increases because commonly encountered NAPLs have a low dielectric permittivity of 2 to 10 vs. 81 for water (Haridy et al., 2004). Similar effects may also be observed with reference to EC_b (Persson and Berndtsson 2002; Comegna et al., 2019). In the selected studies (see Table 1) it was clearly demonstrated that the TDR technique exhibited sufficient sensitivity and resolution for characterization of NAPL volumes in contaminated soils. However, some difficulties in NAPL evaluation via TDR may arise from the fact that the TDR technique supplies the dielectric permittivity of the medium in terms of "global response" which means that measured ε_b depends on the total volume of the distinct phases involved (including NAPL). Therefore TDR cannot directly discriminate the presence of NAPL (Comegna et al., 2016). Furthermore, since the dielectric permittivity of most common NAPLs is similar to that of mineral particles (ε_s=3-7) and air (ε_a=1), under certain conditions (e.g., at low water content), NAPL presence may be confused with the dielectric response of a dry soil (Zhan et al., 2013). Besides, the relationship between the dielectric permittivity of the contaminated soil and θ_{NAPL} is not univocal, in the sense that a given observed permittivity corresponds to different volumetric combinations of water and NAPL. Thus, even if both ε_b and θ_w are available, θ_{NAPL} cannot be inferred without additional information on the distribution of the fluid phase in the soil (Persson and Berndtsson, 2002). Finally, from a physical point of view, the presence of NAPLs in soil contributes to complicate transport equations and interpretative dielectric models because a new phase is introduced, which furthermore can be liquid (immiscible and dissolved) and volatile. In the subsections below the approaches that scientists used to overcome such difficulties are described, as well as their main outcomes.

Table 1
NAPL studies in soils based on the TDR technique.

Refs.	Soil	Saturated/ Unsaturated	Contaminant	Lab/Field
Chenaf and Amara, 2001	Repacked	Saturated	DNAPL	Laboratory
Persson and Berndtsson, 2002	Repacked	Saturated	LNAPL	Laboratory
Haridy et al., 2004	Repacked	Saturated Unsaturated	LNAPL	Laboratory
Mohamed and Said, 2005	Repacked	Saturated	LNAPL x 2 DNAPL x 2	Laboratory
Rinaldi and Francisca, 2006	Repacked	Saturated	LNAPL x 2	Laboratory
Moroizumi and Sasaki, 2008	Repacked	Saturated	LNAPL	Laboratory
Olchawa and Kumor, 2008	Repacked	Unsaturated	DNAPL	Laboratory
Haridy et al., 2011	Repacked	Saturated	LNAPL	Laboratory
Francisca and Montoro, 2012	Repacked	Saturated	LNAPL	Laboratory
Comegna et al., 2013a	Repacked	Saturated	LNAPL	Laboratory
Comegna et al., 2013b	Repacked	Unsaturated	LNAPL	Laboratory
Zhan et al., 2013	Repacked	Unsaturated	LNAPL	Laboratory
Zhan et al., 2014	Repacked	Unsaturated	DNAPL	Laboratory
Comegna et al., 2016	Repacked	Unsaturated	LNAPL	Laboratory
Comegna et al., 2017	Repacked	Unsaturated	LNAPL	Laboratory
Comegna et al., 2019	Repacked	Saturated	LNAPL	Laboratory

5.1. NAPL monitoring in homogeneous, variable saturated soils

Looking at the available research in the literature, a first attempt to monitor NAPL in soils using the TDR technique was made by Chenaf and Amara (2001). The authors prepared 10 soil samples at a constant water content and at three different diesel concentrations. The TDR response of clean and contaminated samples was recorded and analyzed. They observed an effect of the NAPL (they used diesel oil) on the shape of the TDR signal, which is more evident as the NAPL concentration increased. They also showed that to better quantify such changes in the TDR waveforms, the signal amplitude (i.e., the value, at a fixed time, of the reflection coefficient) of the NAPL contaminated signal has to be re-scaled, at each instant, by the amplitude of diesel-free waveforms (Fig. 2). In this manner the output curve appeared as a succession of regularly spaced peaks with decreasing amplitude. Amplitudes of the peaks depend on the diesel concentration.

Other noteworthy results were attained by Persson and Berndtsson (2002) who investigated the influence of light NAPLs (they selected a sunflower seed oil, an n-paraffin oil and a synthetic motor oil) on TDR measurements in a homogeneous silica sand, under saturated and unsaturated flow conditions. The authors developed a method (two-step method) that permitted the NAPL concentration in soils to be determined by interpreting ε_b and EC_b measurements. Their findings (obtained from a series of laboratory batch tests) are summarized in Fig. 3a and b where, at a fixed θ_w=0.10, the measured ε_b and EC_b are plotted against known θ_{NAPL}.

Fig. 4 shows the actual versus estimated θ_{NAPL}. The above authors obtained a coefficient of determination R^2=0.92 and a root mean square error of 0.031 cm^3/cm^3; they also observed that the relative error in the θ_{NAPL} estimate increases at lower NAPL amounts. This may be due to the fact that in almost dry soils, the dielectric response of an NAPL-contaminated medium becomes similar to that of an uncontaminated soil due to the low dielectric permittivity of air and soil mineral grains (Alharthi et al., 1986; Ajo-Franklin et al., 2006).

The proposed two-step approach requires detailed calibration datasets to characterize the dielectric response for a full range of NAPL concentrations (i.e., from dry to saturated soil conditions), which restricts the applicability of the method to laboratory-controlled experiments in homogeneous materials.

The two-step method described by Persson and Berndtsson (2002) was subsequently tested by Haridy et al. (2004) who conducted new

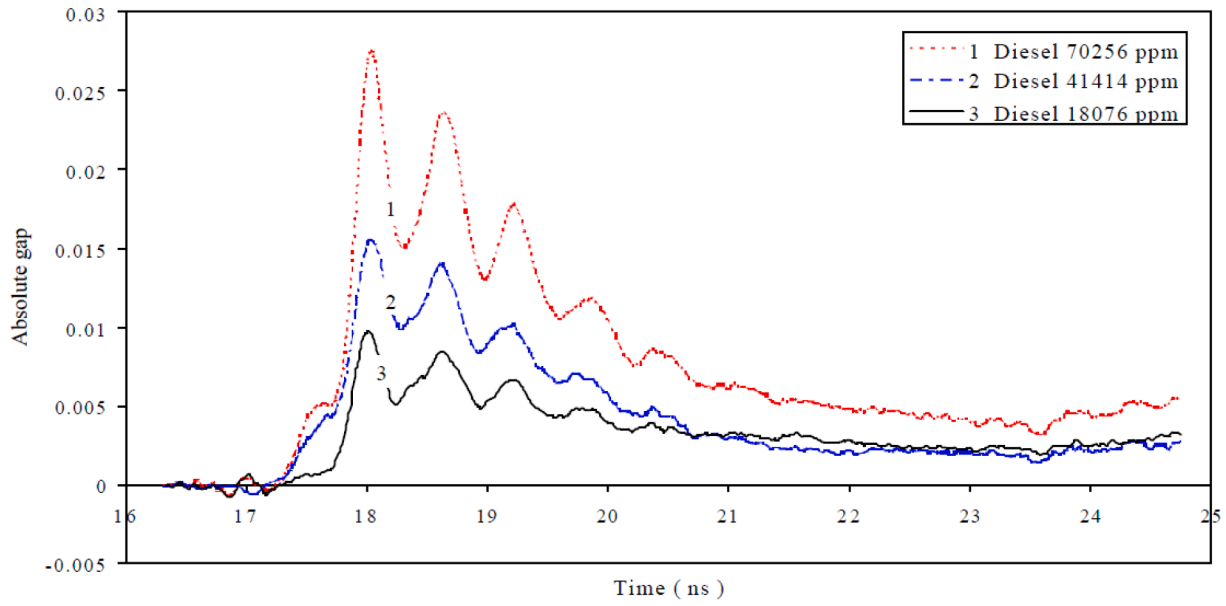

Figure 2

Fig. 2. Differences in TDR signal amplitude calculated between diesel and clean (considered as reference) soil samples versus time (from Chenaf and Amara, 2001).

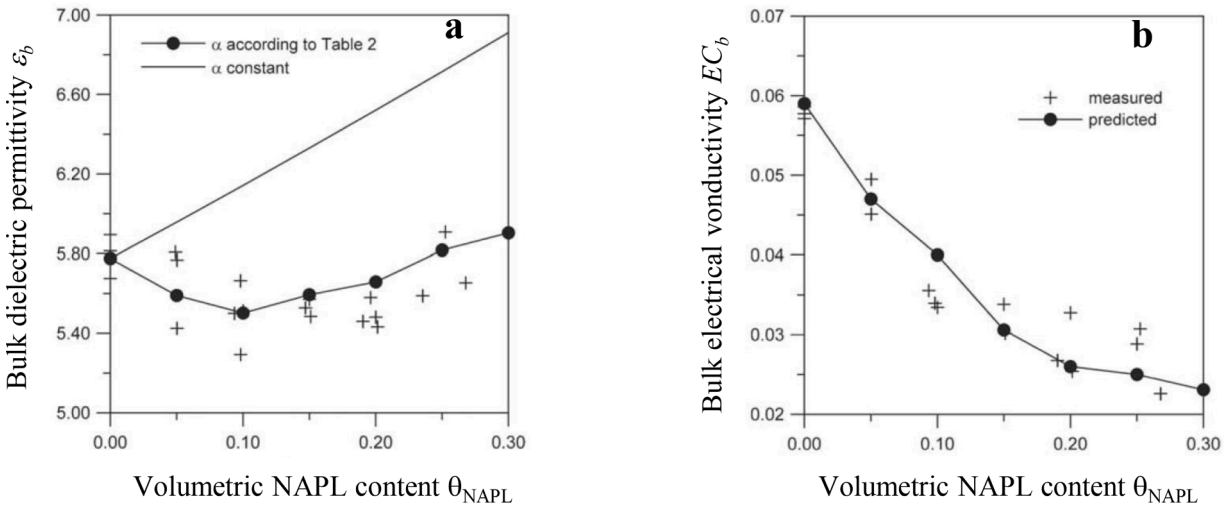

Fig. 3. Measured (a) bulk dielectric permittivity ε_b, and (b) bulk electrical conductivity EC_b versus known volumetric NAPL content θ_{NAPL} in a contaminated silica sand at a fixed θ_w=0.10 (adapted from Persson and Berndtsson, 2002).

laboratory NAPL experiments (in both saturated and unsaturated soils). The authors observed that the two-step method was inaccurate in the case of the fine sand used in their tests since no correlation was observed between θ_{NAPL} and EC_b. They also observed, in most cases, an almost linear relationship between θ_{NAPL} and ε_b.

As the two-step method is not applicable, a different approach was introduced in their study using direct measurements of ε_b and EC_b. Similarly to Persson and Berndtsson (2002), the procedure is based on two distinct steps. In the first step, the water content θ_w is predicted using EC_b measurements (as only water has a major impact on EC_b):

$$\theta_w = 33.45EC_b^3 - 19.37EC_b^2 + 4.43EC_b - 0.1233 \quad (18)$$

Accurate estimates of θ_w were observed (R^2=0.99). Knowledge of θ_w allowed, in the second step, θ_{NAPL} to be determined, using the fact that changes in ε_b depend on changes in both θ_w and θ_{NAPL}. The authors assumed that the bulk dielectric permittivity of the contaminated medium can be written as:

$$\varepsilon_b = \varepsilon_{swa} + \varepsilon_{saNAPL} \quad (19)$$

where, in the current approach, ε_{swa} can be determined by using a third-order polynomial equation as follows:

$$\varepsilon_{swa} = -201.5\theta_w^3 + 151.54\theta_w^2 + 10.10\theta_w + 2.65 \quad (20)$$

It may be noted that the constant terms in Eq. (20) are soil-dependent. Again, in their study, the calculated R^2 is equal to 0.99.

Having determined the effect of water on ε_b, it is possible, from Eq. (19), to extrapolate the NAPL effect(i.e., $\varepsilon_{saNAPL} = \varepsilon_b - \varepsilon_{swa}$) on ε_b and thus to obtain θ_{NAPL} by using as a second-order polynomial equation:

$$\theta_{NAPL} = D_1^3\varepsilon_{saNAPL} + D_2\varepsilon_{saNAPL}^2 + D_3\varepsilon_{saNAPL} + D_4 \quad (21)$$

where D_1, D_2, D_3 and D_4 are soil-dependent parameters, also depending on the soil saturation (i.e., on θ_w). Table 2 reports D values obtained for different θ_w values in the soil under study.

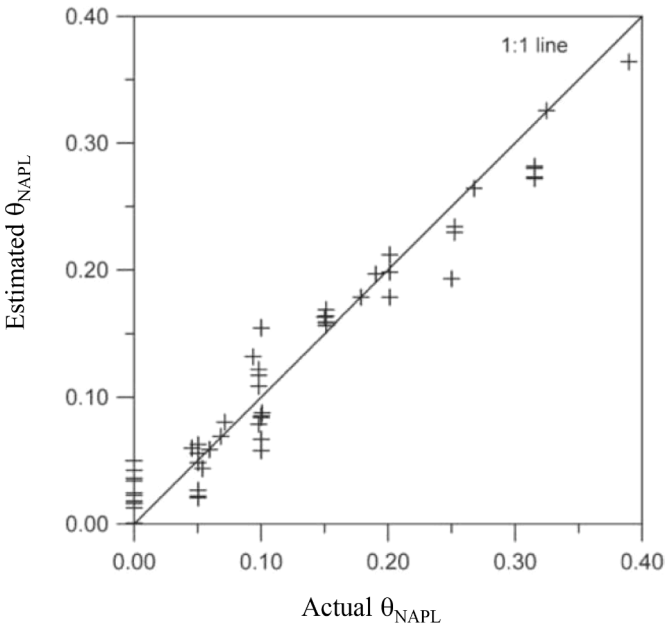

Fig. 4. Estimated versus actual θ_{NAPL} (adapted from Persson and Berndtsson, 2002).

Table 2
Parameters D_1, D_2, D_3 and D_4 and coefficient of determination R^2 of Eq. (21) (from Haridy et al., 2004).

θ_w	D_1	D_2	D_3	D_4	R^2
0	-4.3814	5.0648	-0.9878	0.1116	0.97
0.05	-0.0142	0.3639	0.0251	0.0470	0.99
0.10	0.5925	-1.4027	1.2959	-0.2269	0.96
0.15	-0.0647	0.1217	0.1092	0.0325	0.98

Another interesting paper on the NAPL-TDR topic was published by Haridy et al. (2011). In this study, the authors tackled the problem of mapping NAPL dynamics via the TDR technique in a 2-D multi-fluid flow experiment. A box of 0.45 m x 0.54 m x 0.2 m was prepared with a fine sandy soil. An NAPL mixed with a dye tracer was applied in four releases at the top of the container from a rectangular source placed in the middle of the soil surface. In addition to the NAPL, at a certain time during the test, a saline water solution and tap water were added to the soil, and their dynamics were monitored with time. In all, 42 three-rod TDR probes were installed to detect the transport and the location of the different fluids in the investigated soil domain, via ε_b and EC_b measurements. In addition to the TDR measurements, NAPL migration was also monitored by means of imaging analysis using a digital camera. Estimates of NAPL amounts in the soil were obtained using Eq. (21), implemented with the parameters of Table 2.

The authors concluded that the multi-channelled experiment supplied detailed data about the migration of the NAPL with an adequate spatio-temporal resolution. Overall, the results showed good agreement between the propagation and location of the NAPL detected via TDR and digital imaging analysis. The multi-channelled TDR system can be considered a good tool for quantitative analysis describing NAPL movement in soils.

Francisca and Montoro (2012) published the results of a series of NAPL experiments conducted in soils of different textures, using paraffin oil as a contaminant. Their findings were used to calibrate and validate the dielectric mixing model of Eq. (17), in which parameter α was fixed at 0.5 (i.e., the soil was considered isotropic and homogeneous).

Fig. 5a shows the dependence of the volumetric fluid content θ_f over the dielectric permittivity of the contaminated medium for different β values, which were varied between 0 and 1 (with steps of 0.25). Fig. 5b shows the performance of the dielectric model in terms of the volumetric NAPL content computed from Eq. (17), and the known θ_{NAPL} content obtained from an independent data set specifically acquired for model validation. The authors observed that, due to the complexity of the contaminated soil system, the dielectric permittivity of NAPL-contaminated soils is influenced by several factors such as soil porosity, volumetric content of water and NAPL, degree of soil saturation, as well as the dielectric permittivity values, at saturation, of the fully cleaned and the fully contaminated soils.

In any case, once the initial and boundary conditions of the contaminated system are defined, it is possible to estimate NAPL contents from dielectric permittivity measurements with acceptable accuracy (R^2>0.90).

The limit of this approach, and in general of the approaches described above, is that it requires calibration curves relating the dielectric permittivity and the volumes of fluids θ_f (i.e., water+NAPL) to be constructed for specific soil texture and porosity conditions.

Finally, Comegna et al. (2016) proposed a different approach for

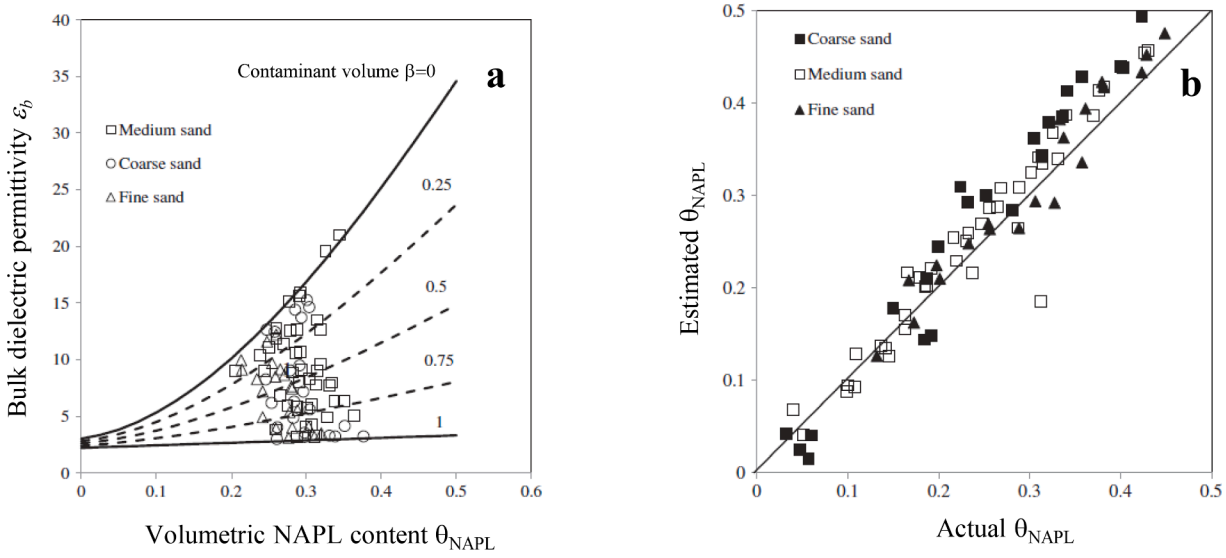

Fig. 5. a) Bulk dielectric permittivity ε_b of water-paraffin oil-sand mixtures versus known volumetric fluid content θ_f, b) estimated and actual θ_{NAPL} content (adapted from Francisca and Montoro 2012).

estimating NAPL content in variably saturated soils. The new approach is based on the interpretation of TDR signals of an NAPL-contaminated medium in two different time domains (i.e., $t \cong 25$ ns and $t \cong 507$ ns). At the different observation time-windows, TDR waveforms generate systematic and time-specific dielectric responses that only depend on the amount of NAPL in the porous medium. The authors demonstrated that the final value of the reflection coefficient ρ_f (i.e., the ρ value acquired at long times from the wave generator) can be univocally related with θ_{NAPL} through the following equation (based on a rewrite of the dielectric α mixing model of Eq. (12); for more details see Comegna et al., 2016):

$$\theta_{NAPL} = \frac{(1-\phi)\varepsilon_s^\alpha + \phi\varepsilon_a^\alpha + \left(a_c\rho_f + \left(b_1\varepsilon_b^\alpha + b_2\varepsilon_b^\alpha + b_3\right)\right)\left(\varepsilon_w^\alpha - \varepsilon_a^\alpha\right) - \varepsilon_b^\alpha}{\varepsilon_w^\alpha - \varepsilon_{NAPL}^\alpha} \tag{22}$$

where b_1, b_2 b_3 and a_c are soil-dependent fitting parameters. Figs. 6 and 7 illustrate some results of the experiment above described. Fig. 6 reports the acquired TDR waveforms at different times. Fig. 7 shows, in a 1:1 plot, the volumetric NAPL content computed from Eq. (22) and the known θ_{NAPL} content with reference to three soils with different textures and pedological characteristics. The authors calculated a model efficiency, *EF*, that lies in the range 0.96 to 0.99, at least in the θ_f domain investigated.

5.2. NAPL monitoring in layered, variable saturated soils

The matter of characterizing the dielectric behaviour of an NAPL-contaminated plume that moves in a layered soil matrix is a further complication to the case of homogeneous soils, that has to date attracted little attention (see e.g., Barnett, 2002; Zhan et al., 2013, 2014; Comegna et al., 2017).

Some authors (Topp et al., 1982; Zhang et al., 2000; Yu and Yu, 2006; Comegna et al., 2017, among others) have observed that when a TDR signal passes through a soil-layer interface, an impedance change occurs with the effect of producing a distinguishable reflection on the TDR waveform. This impedance change may also occur in a homogeneous soil, in the presence of a wetting front, i.e., at the interface between the wet and the dry zone, which from a dielectric point of view behaves as a discontinuity (Topp et al., 1982)

Following these considerations, Zhan et al. (2013) and (2014) conducted a series of well-organized and detailed laboratory experiments

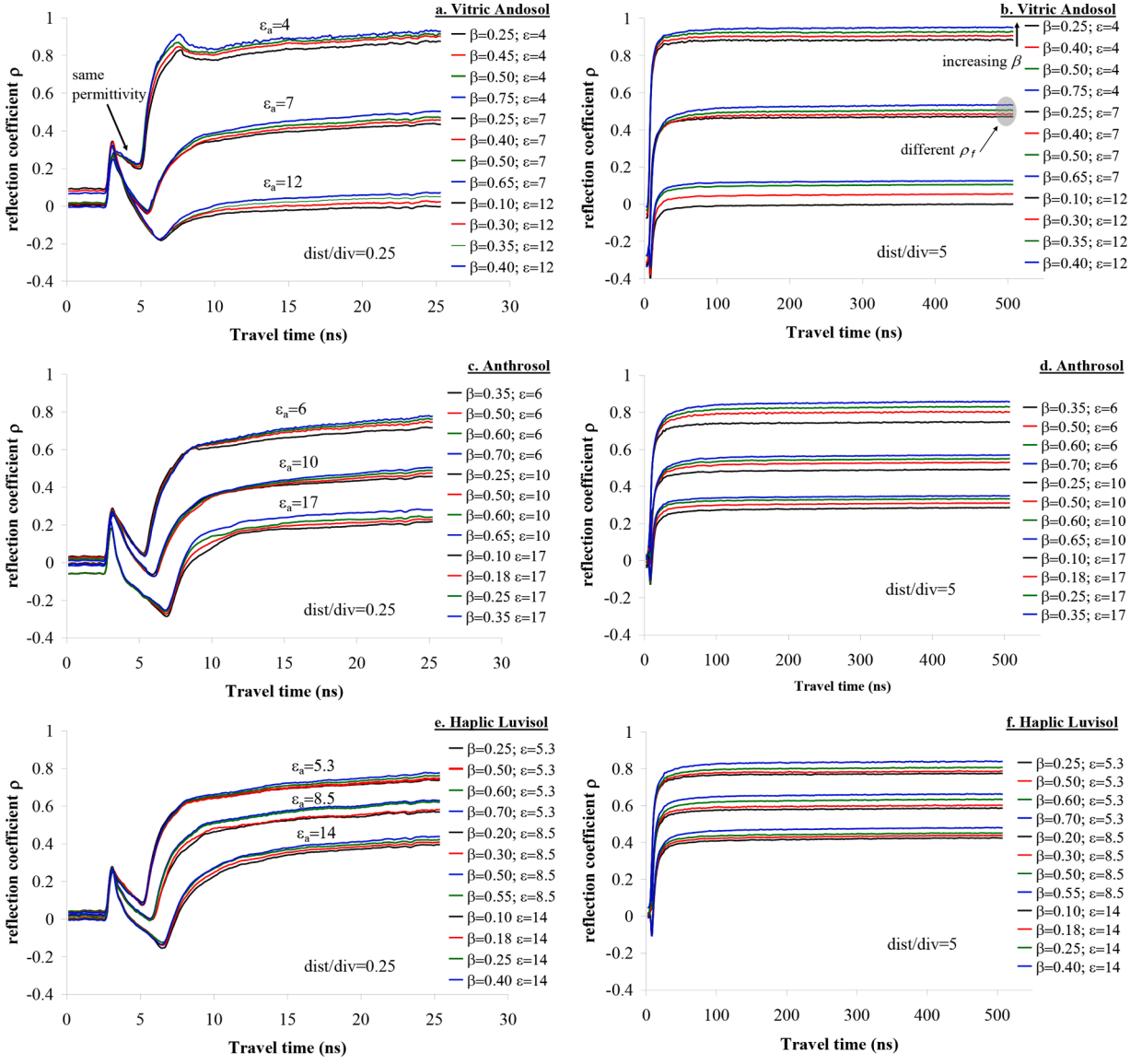

Fig. 6. Examples of TDR waveforms captured at two observation windows (i.e., time t=25.37 ns and t=507.42 ns), for different levels of contamination β (from Comegna et al., 2016).

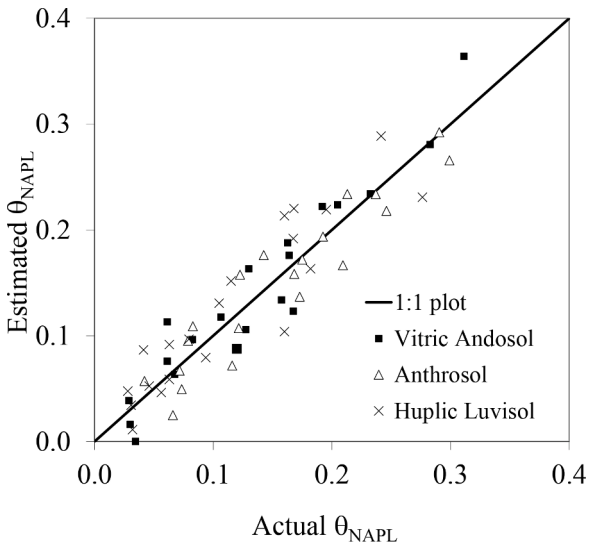

Fig. 7. Estimated (Eq. (22)) versus actual θ_{NAPL} content of contaminated soils (adapted from Comegna et al., 2016).

aiming to systematically investigate the effects on TDR signals of NAPL layers embedded in soils. These effects were studied by arranging an experimental layout in which a diesel-contaminated layer was sandwiched between (i) two dry sand layers, (ii) two water-saturated sand layers, and (iii) a dry sand layer and a water-saturated sand layer. The effect of the thickness of each single layer on the shape of the TDR signal was also analyzed to predict the height of each single layer.

They concluded that their methodology may facilitate NAPL detection in contaminated sites in all the investigated cases except where the NAPL layer is embedded between two dry sand layers. Indeed, in this scheme, NAPL cannot be identified because the dielectric changes at the different layer interfaces are indistinguishable.

Topp et al. (1982) demonstrated that a wetting front moving in a soil profile can be detected by the TDR method. According to Topp's approach, in a soil with two layers, namely i and j, each with its own dielectric permittivity, ε_{bi} and ε_{bj}, and wave travel time, t_i and t_j, the partial length L_i (i.e., the length of the wetting front) of the transmission line in the i-th layer can be approximated by:

$$L_i = \frac{ct_i}{\sqrt{\varepsilon_{bi}}} \tag{23}$$

and the complementary length, L_j, in layer j may be determined as:

$$L_j = L - L_i \tag{24}$$

where L is the total length of the transmission line (i.e., the probe length). In the case of a NAPL contaminated front L_i=L_{NAPL}.

Eq. (23), accordingly to Zhan et al. (2013), can be applied in all those situations where a dielectric discontinuity is distinguishable across the NAPL front.

Comegna et al., (2017), starting from Zhan's et al. (2014) results, proposed an innovative formulation for NAPL front detection in soils, that allows the NAPL front location in a soil profile to be estimated even in those situations in which the TDR waveform does not clearly show

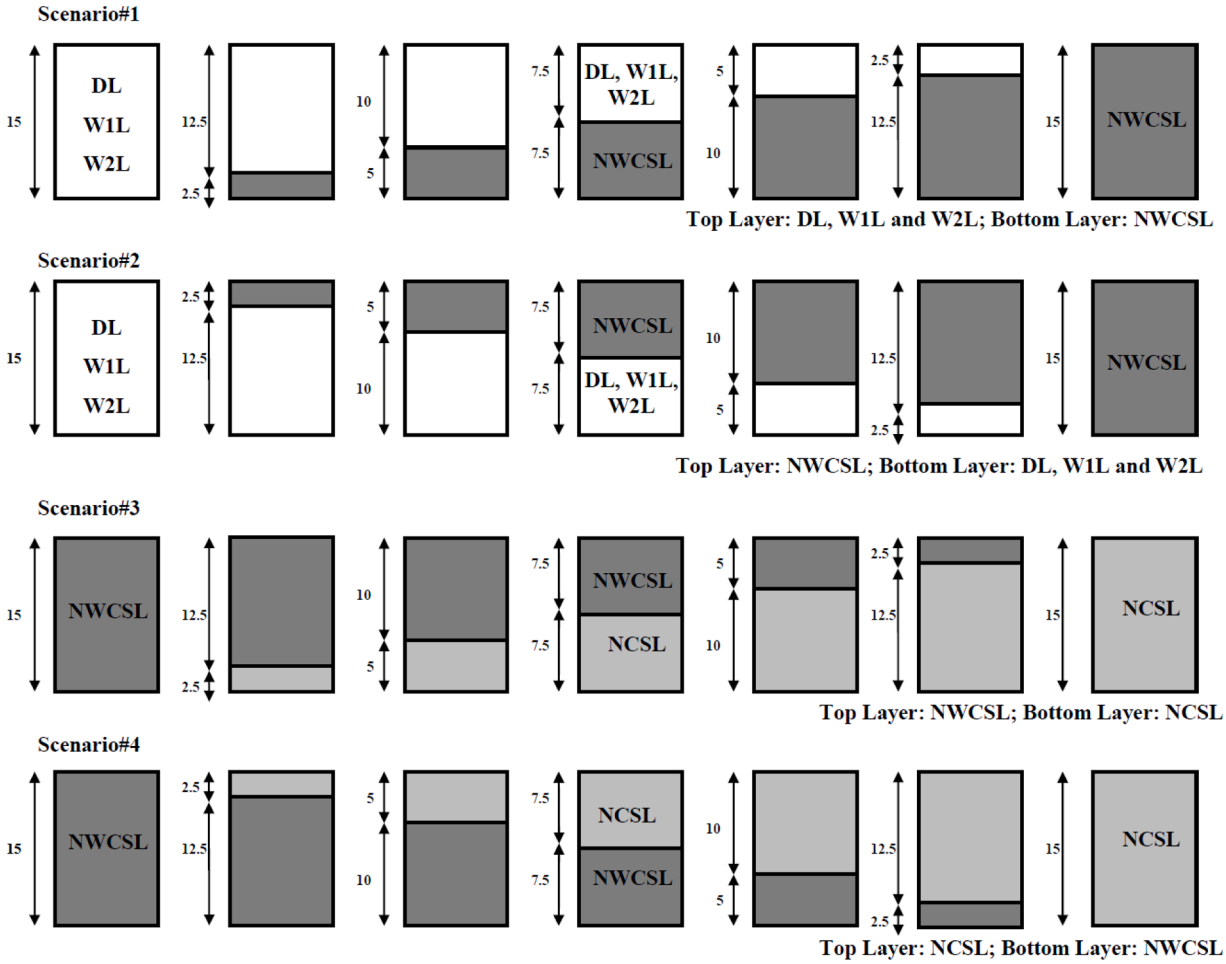

Fig. 8. Experimental layout for contaminated soil layers simulating the NAPL front (units in centimetres; from Comegna et al., 2017).

any evident reflection at the front interface. The methodology is based on TDR signal analysis, coupled with EC_b measurements. The authors implemented a full factorial series of laboratory-controlled tests, based on the experimental framework of Fig. 8, in which four distinct scenarios of practical interest are proposed. In scenario 1, the authors simulated a condition where, at the beginning, a soil sample was completely dry (dry layer, DL) or at a uniform water content (water-soil layer with volumetric water content of: 0.20, W1L; and 0.30, W2L). At a certain point, it was assumed that the NAPL was applied at the sample bottom (NAPL+water contaminated soil layer, NWCSL layer), such that the front moved upward. In scenario 2, the initial condition was similar to that of scenario 1, but now the NAPL source (i.e., NWCSL layer) propagated downward. In the last two scenarios (3 and 4), at the beginning soil samples were originally NAPL-contaminated. In these two cases it was assumed that the water fraction (NAPL contaminated soil layer, NCSL layer) gradually leaves the soil sample from the bottom (scenario 3) and from the top (scenario 4) of the soil profile.

The authors stated that the position of the NAPL contaminant front can be calculated as a linear function of EC_b:

$$L_{NAPL} = aEC_b + b \tag{25}$$

where a and b are soil-dependent coefficients that depend on θ_{NAPL} and θ_w (see Table 2 of Comegna et al., 2017).

Fig. 9 shows the relative error (E_{rel}), calculated as the normalized difference between predicted (with Eqs. (23) and (25)) and observed data. E_{rel} varies between -0.74 and 1.17 (Eq. (23)) and -0.41 and 0.24 (Eq. (25)), which indicates the satisfactory agreement of the proposed Eq. (25).

5.3. NAPL monitoring during soil decontamination processes

Rinaldi and Francisca (2006) arranged a laboratory study to measure the dielectric permittivity of NAPL-contaminated sands during a decontamination process. For the tests, they used paraffin oil and lubricant oil as a contaminant, and four different washing solutions (i.e., deionized water, a water-detergent solution, a water-detergent-alcohol solution, and water vapour). The main results of the research are shown in Fig. 10a, b. They demonstrated the efficiency of the applied remediation solutions but also the possibility to infer the stage of remediation from permittivity measurements.

On the same topic, Comegna et al. (2013a), and (2019) developed an extensive dataset of NAPL contamination-decontamination laboratory experiments. The authors used corn oil as a contaminant and three washing solutions (*ws*) for soil cleaning. The washing solutions were obtained by mixing different amounts of water, a commercial detergent and methanol. The main aim of the experiments was to sustain the outcome of Rinaldi and Francisca's (2006) tests, and in addition to quantitatively predict, *"in real time"*, the presence of the NAPL within the soil during the decontamination stage. To achieve the above results, the authors, using two distinct datasets, calibrated and validated the dielectric mixing model of Eq. (12) which, for a fully saturated medium (i.e., $\theta_f = \phi$), can be rewritten as (for more details see Comegna et al., 2019):

$$\theta_{NAPL} = \frac{(1-\phi)\varepsilon_s^\alpha + \phi\varepsilon_{ws}^\alpha - \varepsilon_b^\alpha}{\varepsilon_{ws}^\alpha - \varepsilon_{NAPL}^\alpha} \tag{26}$$

From Eq. (26), θ_{NAPL} can be estimated during the progression of the soil decontamination if the soil porosity ϕ and the dielectric permittivity of the soil-washing solution-NAPL mixture (i.e., ε_b) are known; ε_b is measurable via TDR. Eq. (26) also requires a priori knowledge of the dielectric permittivities of the NAPL (ε_{NAPL}) and the washing solutions (ε_{ws}).

Fig. 11 shows a selection of observed and estimated θ_{NAPL} versus dielectric permittivity of the multiphase system (i.e., soil-NAPL-washing solution) with reference to the different washing solutions (namely wd, wda#1, wda#2; for more details see Comegna et al., 2019) used during the remediation tests. The authors observed the high performance of the developed model to evaluate the residual NAPL content in the soil samples. The calculated model efficiency, *EF*, statistical index was high, with mean values greater than 0.90. Overall, quantitative evaluations reveal the suitability of the dielectric model adopted to estimate the volumetric NAPL content in the θ_{NAPL} range 0.15-0.40 (Table 3).

6. Conclusions

In this paper, we proposed a state-of-the-art overview of the use of TDR technology in monitoring non-miscible contaminants in variably saturated soils. With reference to this research topic, interesting papers have been published in international journals with an increasing number of interested readers over the years. These papers, as shown in section 5, deal with the theme of NAPL monitoring in homogeneous and heterogeneous soils, under variable saturated conditions. Several studies also focused on the problem of NAPL monitoring during soil decontamination processes.

The documented research is based on extensive laboratory experiments developed to fully explore and investigate, from a dielectric point of view, the complexity of multiphase soil systems contaminated with NAPLs. From this complexity, to discriminate NAPL volumes among other phases involved, the authors proposed different approaches that

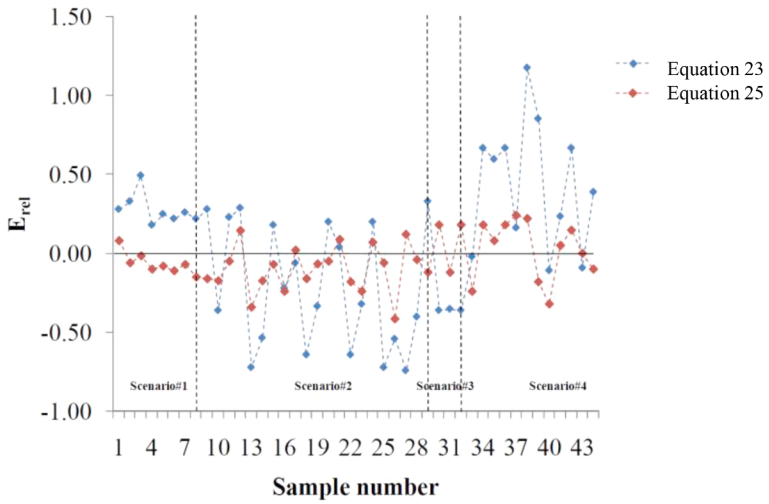

Fig. 9. Relative error E_{rel} of Eqs. (23) and (25) computed for the four investigated scenarios (from Comegna et al., 2017).

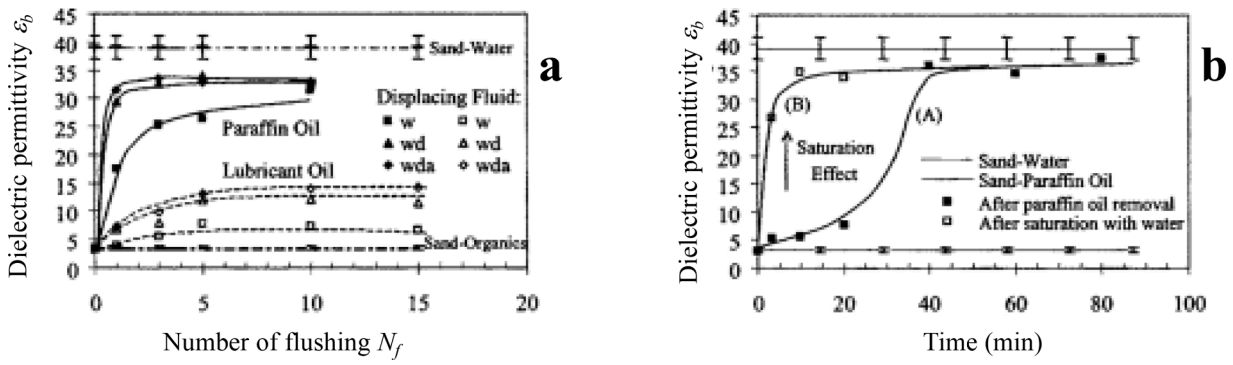

Fig. 10. a) Measured dielectric permittivity ε_b versus the number of flushings N_f of sand contaminated with paraffin oil, and lubricant oil: w=water, wd=water-detergent, and wda=water-detergent-alcohol, b) measured dielectric permittivity ε_b versus time of sand contaminated with paraffin oil remediated with water vapour (adapted from Rinaldi and Francisca, 2006).

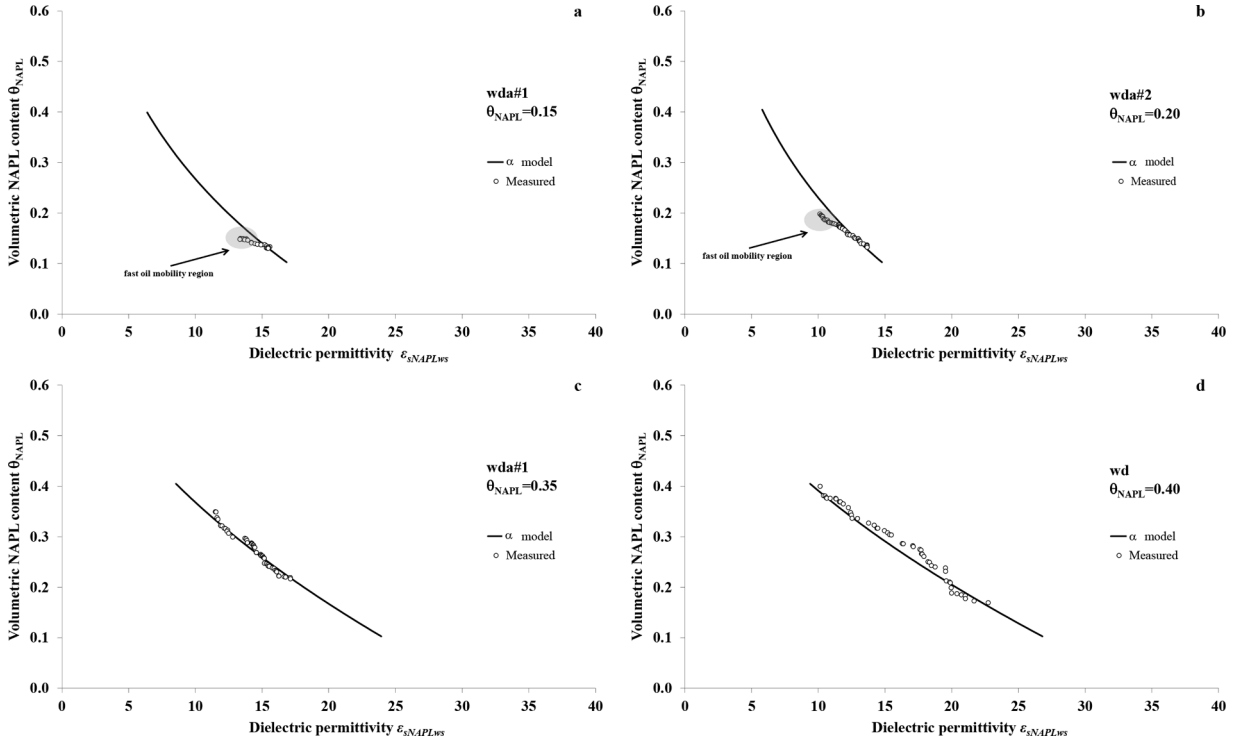

Fig. 11. Selection of measured (symbols) and modelled (dashed lines) volumetric NAPL content versus dielectric permittivity of soil samples saturated with NAPL and washing solution ($\varepsilon_{sNAPLws}$), with reference to the different washing solutions (wd, wda#1 and wda#2) used during the remediation tests (Comegna et al., 2019).

Table 3
Model efficiency (EF) and mean bias error (MBE) statistical indices, referring to measured and predicted (Eq. (26)) θ_{NAPL} (cm^3/cm^3), calculated in the range of model applicability ($0.15<\theta_{NAPL}<0.40$).

Washing solution	θ_{NAPL}=0.15		θ_{NAPL}=0.20		θ_{NAPL}=0.25	
	EF	MBE	EF	MBE	EF	MBE
wd	0.98	1.548	0.93	-0.422	0.96	0.570
wda no.1	0.86	0.405	0.99	0.516	0.97	-0.048
wda no.2	0.84	0.148	0.94	0.420	0.66	0001
Washing solution	θ_{NAPL}=0.30		θ_{NAPL}=0.35		θ_{NAPL}=0.40	
	EF	MBE	EF	MBE	EF	MBE
wd	0.98	-0.023	0.99	-0.153	0.99	-0.179
wda no.1	0.95	-0.074	0.99	-0.066	0.99	0.303
wda no.2	0.91	0.014	0.97	0.326	0.99	0.019

are mainly based on the use of dielectric mixing models. Such models, if adequately calibrated and validated, allow NAPLs to be quantitatively detected in contaminated media.

The different methodologies proposed and described in the present paper can be considered a notable contribution to NAPL detection in contaminated soils via TDR. However, there are still some intrinsic limitations in the proposed research works that should be overcome to consolidate the results so far obtained. Indeed, the procedures described require further experiments and data sets, especially at a full field-scale, to explore the physical basis of complex soil-NAPL interactions in different pedological contexts, and to evaluate the performance of the proposed approaches under real field conditions.

CRediT authorship contribution statement

Alessandro Comegna: Conceptualization, Methodology, Writing – original draft. **Gerardo Severino:** Conceptualization, Methodology,

Writing – original draft. **Antonio Coppola:** Conceptualization, Methodology, Writing – original draft.

Declaration of Competing Interest

The authors declare that they have no known competing financial interests or personal relationships that could have appeared to influence the work reported in this paper.

Data availability

The authors are unable or have chosen not to specify which data has been used.

References

Ajo-Franklin, J.B., Geller, J.T., Harris, J.M., 2006. A survey of the geophysical properties of chlorinated DNAPLs. J. Appl. Geophys. 59, 177–189. https://doi.org/10.1016/j.jappgeo.2005.10.002.

Alharthi, A., Lange, J., Whitaker, E., 1986. Immiscible fluid flow in porous media: dielectric properties. J. Contam. Hydrol. 1, 107–118. https://doi.org/10.1016/0169-7722(86)90010-0.

Barnett, D.A., 2002. Detection of diesel fuel leakage from underground tank using time domain reflectometry. M.S. thesis. Northwest Missouri State Univ., Maryville.

Birchak, J.R., Gardner, C.Z.G., Hipp, J.E., Victor, J.M., 1974. High dielectric constant microwave probes for sensing soil moisture. Proc. IEEE 62, 93–98. https://doi.org/10.1109/PROC.1974.9388.

Carpena, R.M., Regalado, C.M., Ritterb, A., Alvarez-Benedi, J., Socorro, A.R., 2005. TDR estimation of electrical conductivity and saline solute concentration in a volcanic soil. Geoderma 124, 399–413.

Chenaf, D., Amara, N., 2001. Time domain reflectometry for the characterization of diesel contaminated soils. In: Proceedings of the 2nd International Symposium and Workshop on Time Domain Reflectometry for Innovaztive Geotechnical Applications (5-7 September 2001). Infrastructure Technology Institute, Northwestern University, Evanston, Illinois, USA.

Comegna, V., Coppola, A., Sommella, A., 1999. Nonreactive solute transport in variously structured soil materials as determined by laboratory-based time domain reflectometry (TDR). Geoderma 92, 167–184.

Comegna, V., Coppola, A., Sommella, A., 2001. Effectiveness of equilibrium and physical non-equilibrium approaches for interpreting solute transport through undisturbed soil columns. J. Contam. Hydrol. 50, 121–138. https://doi.org/10.1016/S0169-7722(01)00100-0.

Comegna, V., Coppola, A., Comegna, A., 2011. Laboratory-scale study on reactive contaminant transport in soil by means of one-dimensional advective dispersive models. J. Agric. Eng. 3, 1–6.

Comegna, A., Coppola, A., Sommella, A., Vitale, C., 2003. Scale dependence of local water fluxes and solute transport in a field soil. Giornata di Studio: Metodi Statistici e Matematici per le Analisi Idrologiche, Rome 2003.

Comegna, A., Coppola, A., Dragonetti, G., Sommella, A., 2013a. Dielectric response of a variable saturated soil contaminated by non-aqueous phase liquids (NAPLs). Procedia Environ. Sci. 19, 701–710.

Comegna, A., Coppola, A., Dragonetti, G., Chaali, N., Sommella, A., 2013b. Time domain reflectometry-measuring dielectric permittivity to detect soil non-aqueous phase liquids contamination-decontamination processes. In: J. Agric. Eng., XLIV, p. e167.

Comegna, A., Coppola, A., Dragonetti, G., Severino, G., Sommella, A., Basile, A., 2013c. Dielectric properties of a tilled sandy volcanic-vesuvian soil with moderate andic features. Soil Till. Res. 133, 93–100. https://doi.org/10.1016/j.still.2013.06.003.

Comegna, A., Coppola, A., Dragonetti, G., Sommella, A., 2016. Estimating non-aqueous phase liquid (NAPL) content in variable saturated soils using time domain reflectometry (TDR). Vadose Zone J. https://doi.org/10.2136/vzj2015.11.0145.

Comegna, A., Coppola, A., Dragonetti, G., Sommella, A., 2017. Interpreting TDR signal propagation through soils with distinct layers of nonaqueous-phase liquid and water content. Vadose Zone J. https://doi.org/10.2136/vzj2017.07.0141.

Comegna, A., Coppola, A., Dragonetti, G., 2019. A soil non-aqueous phase liquid (NAPL) flushing laboratory experiment based on measuring the dielectric properties of soil–organic mixtures via time domain reflectometry (TDR). Hydrol. Earth Syst. Sci. 23, 3593–3602. https://doi.org/10.5194/hess-23-3593-2019.

Comegna, A., Coppola, A., Dragonetti, G., 2020. Time domain reflectometry for dielectric characterization of olive mill wastewater contaminated soils. J. Agric. Eng. 1092, 248–254. https://doi.org/10.4081/jae.2020.1092.

Coppola, A, Comegna, V, Basile, A, Lamaddalena, N, Severino, G., 2009. Darcian preferential water flow and solute transport through bimodal porous systems: experiments and modelling. J. Hydrol. Contam. https://doi.org/10.1016/j.jconhyd.2008.10.004.

Coppola, A., Comegna, A., Dragonetti, G., Dyck, M., Basile, A., Lamaddalena, N., Comegna, V., 2011a. Solute transport scales in an unsaturated stony soil. Adv. Water Resour. 34, 747–759.

Coppola, A., Comegna, A., Dragonetti, G., Lamaddalena, N., Kader, A.M., Comegna, V., 2011b. Average moisture saturation effects on temporal stability of soil water spatial distribution at field scale. Soil Till. Res. 114, 155–164.

Coppola, A., Gerke, H.H., Comegna, A., Basile, A., Comegna, V., 2012. Dual-permeability model for flow in shrinking soil with dominant horizontal deformation. Water Resour. Res. 48, W08527. https://doi.org/10.1029/2011WR011376.

Coppola, A., Dragonetti, G., Comegna, A., Lamaddalena, N., Caushi, B., Haikal, M.A., Basile, A., 2013. Measuring and modeling water content in stony soils. Soil Till. Res. 128, 9–22.

Comegna, A., Dragonetti, G., Kodesova, R., Coppola, A., 2022. Impact of olive mill wastewater (OMW) on the soil hydraulic and solute transport properties. Int. J. Environ. Sci. Technol. https://doi.org/10.1007/s13762-021-03630-6.

Coppola, A., Chaali, N., Dragonetti, G., Lamaddalena, N., Comegna, A., 2015. Root uptake under non-uniform root-zone salinity. Ecohydrology 1363–1379. https://doi.org/10.1002/eco.1594. ISSN: 1936-0584.

Dalton, F.N., Herkelrath, W.N., Rawlins, D.S., Rhoades, J.D., 1984. Time-domain reflectometry: simultaneous measurement of soil water content and electrical conductivity with a single probe. Science 224, 989–990.

De Loor, G.P., 1964. Dielectric properties of heterogeneous mixtures. Appl. Sci. Res. 3, 479–482. https://doi.org/10.1007/BF02919923.

Dirksen, C.E., Dasberg, S., 1993. Improved calibration of time domain reflectometry soil water content measurements. Soil Sci. Soc. Am. J. 57, 660–667.

Dobson, M.C., Ulaby, F.T., Hallikainen, M.T., El-Rayes, M.A., 1985. Microwave dielectric behavior of wet soil-part II: dielectric mixing models. IEEE Trans. Geosci. Remote Sens. GE-23, 35–46.

Dragonetti, G., Comegna, A., Ajeel, A., Deidda, G., Lamaddalena, N., Rodriguez, G., Vignoli, G., Coppola, A., 2018. Calibrating electromagnetic induction conductivities with time-domain reflectometry measurements. Hydrol. Earth Syst. Sci. 22, 1509–1523. https://doi.org/10.5194/hess-22-1509-2018.

Feng, W., Lin, C.P., Deschamps, R.J., Drnevich, V.P., 1999. Theoretical model of a multisection time domain reflectometry measurement system. Water Resour. Res. 35 (8), 2321–2331.

Francisca, M., Montoro, M.A., 2012. Measuring the dielectric properties of soil-organic mixtures using coaxial impedance dielectric reflectometry. J. Appl. Geophys. 80, 101–109.

Giese, K., Tiemann, R., 1975. Determination of the complex permittivity from thin-sample time domain reflectometry: improved analysis of the step response waveform. Adv. Mol. Relax. Process. 7, 45–49.

Haridy, S.A., Persson, M, Berndtsson, R., 2004. Estimation of LNAPL saturation in fine sand using time-domain reflectometry. Hydrol. Sci. 49, 987–1000.

Haridy, S.A., Persson, M., Berndtsson, R., 2011. Mapping of non-aqueous phase liquids using time domain reflectometry. Vatten 67, 123–130.

Heimovaara, T.J., 1994. Frequency domain analysis of time domain reflectometry waveforms: 1. Measurements of the complex dielectric permittivity of soils. Water Resour. Res. 30 (2), 189–199.

Hilhorst, M.A., 1998. Dielectric characterisation of soil. Ph.D. diss. Wageningen Agric. Univ., Wageningen, the Netherlands.

Hilhorst, M.A., 2000. A pore water conductivity sensor. Soil Sci. Soc. Am. J. 64, 1922–1925.

Huisman, J.A., Lin, C.P., Weihermuller, L., Vereecken, H., 2008. Accuracy of bulk electrical conductivity measurements with time domain reflectometry. Vadose Zone J. 7, 426–433.

Jones, S.B., Wraith, J.M., Or, D., 2002. Time domain reflectometry measurement principles and applications. Hydrol. Process. 16, 141–153.

Kachanoski, R.G., Pringle, E., Ward, A., 1992. Field measurement of solute travel time using time domain reflectometry. Soil Sci. Soc. Am. J. 56, 47–52.

Kraus, J.D., 1984. Electromagnetics, 3rd ed. McGraw-Hill, New York, p. 775.

Lin, C.P., Chung, C.C., Tang, S.H., 2007. Accurate TDR measurement of electrical conductivity accounting for cable resistance and recording time. Soil Sci. Soc. Am. J. 71, 1278–1287.

Lin, C.P., Chung, C.C., Tang, S.H., Huisman, J.A., 2008. Clarification and calibration of reflection coefficient for TDR electrical conductivity measurement. Soil Sci. Soc. Am. J. 72, 1033–1040.

Lin, C.P., Tang, S.H., Lin, C.H., Chung, C.C., 2015. An improved modeling of TDR signal propagation for measuring complex dielectric permittivity. J. Earth Sci. 26 (6), 827–834.

Mallants, D., Vanclooster, M., Meddahi, M., Feyen, J., 1994. Estimating solute transport in undisturbed soil columns using time-domain reflectometry. J. Contam. Hydrol. 17, 91–109.

Mercer, J.W., Cohen, R.M., 1990. A review of immiscible fluids in the subsurface: properties, models, characterization, and remediation. J. Contam. Hydrol. 6, 107–163.

Miyamoto, T., Kameyama, K., Yukiyoshi, I., 2015. Monitoring electrical conductivity and nitrate concentrations in an andisol field using time domain reflectometry. Jpn. Agric. Res. Q. 49, 261–267.

Mohamed, A.M.O., Said, R.A., 2005. Detection of organic pollutants in sandy soils via TDR and eigendecomposition. J. Contain. Hydrol. 76, 235–249.

Mohamed, A.M.O., 2006. Principles and applications of time domain electrometry in geoenvironmental engineering. In: Developments in Arid Region Research, 5. Taylor and Francis.

Mojid, M.A., Hossain, A.B.M.Z., Cappuyns, V., Wyseure, G.C.L., 2016. Transport characteristics of heavy metals, metalloids and pesticides through major agricultural soils of Bangladesh as determined by TDR. Soil Res. 54, 970–984.

Moroizumi, T., Sasaki, Y., 2008. Estimating the nonaqueous-phase liquid content in saturated sandy soil using amplitude domain reflectometry. Soil Sci. Soc. Am. J. 72, 1520–1526.

Nadler, A., Dasberg, S., Lapid, I., 1991. Time domain reflectometry measurements of water content and electrical conductivity of layered soil columns. Soil Sci. Soc. Am. J. 55, 938–943.

Noborio, K., 2001. Measurement of soil water content and electrical conductivity by time domain reflectometry: a review. Comput. Electron. Agric. 31, 213–237.
Noborio, K., Kachanoski, R.G., Tan, C.S., 2006. Solute transport measurement under transient field conditions using time domain reflectometry. Vadose Zone J. 5, 412–418.
Olchawa, A., Kumor, M., 2008. Time domain reflectometry (TDR)-measuring dielectric constant of polluted soil to estimate diesel oil content. Arch. Hydro-Eng. Environ. Mech. 55, 55–62.
Payero, J.O., Tarkalson, D.D., Suat, I., 2006. Use of time domain reflectometry for continuous monitoring of nitrate-nitrogen in soil and water. Biol. Syst. Eng. 53. Papers and Publications. https://digitalcommons.unl.edu/biosysengfacpub/53.
Persson, M., 1997. Soil solution electrical conductivity measurements under transient conditions using time domain reflectometry. Soil Sci. Soc. Am. J. 61, 997–1003.
Persson, M., Berndtsson, R., 1998. Estimating transport parameters in an undisturbed soil column using time domain reflectometry and transfer function theory. J. Hydrol. 205, 232–247.
Persson, M., Berndtsson, R., 2002. Measuring nonaqueous phase liquid saturation in soil using time domain reflectometry. Water Resour. Res. 38 https://doi.org/10.1029/2001WR000523.
Redman, J.D., Kueper, B.H., Annan, A.P., 1991. Dielectric stratigraphy of a DNAPL spill and implications for detection with ground penetrating radar. Ground water monitoring and geophysical methods. In: Proceedings of the 5th National Outdoor Action Conference. Natl. Ground Water Assoc., Las Vegas. Nev.
Regalado, C.M., Munoz-Carpena, R., Socorro, A.R., Hernandez-Moreno, J.M., 2003. Time domain reflectometry models as a tool to understand the dielectric response of volcanic soils. Geoderma 117, 313–330.
Rinaldi, V.A., Francisca, F.M., 2006. Removal of immiscible contaminants from sandy soils monitored by means of dielectric measurements. J. Environ. Eng. 132, 931–939.
Rhoades, J.D., Manteghi, N.A., Shouse, P.J., Alves, W.J., 1989. Soil electrical conductivity and soil salinity: new formulations and calibrations. Soil Sci. Soc. Am. J. 53, 433–439.
Robinson, D.A., Friedman, S.P., 2002. The effective permittivity of dense packing of glass beads, quartz sand and their mixtures immersed in different dielectric backgrounds. J. Non-Cryst. Solids 305, 261–267. https://doi.org/10.1016/S0022-3093(02)01099-2.
Roth, K., Shulin, R., Fluhler, H., Attinger, W., 1990. Calibration of time domain reflectometry for water content measurement using a composite dielectric approach. Water Resour. Res. 26, 2267–2273.
Severino, G., Comegna, A., Coppola, A., Sommella, A., Santini, A., 2010. Stochastic analysis of a field-scale unsaturated transport experiment. Adv. Water. Resour. 33, 1188–1198. https://doi.org/10.1016/j.advwatres.2010.09.004.
Topp, G.C., Davis, J.L., Annan, A.P., 1980. Electromagnetic determination of soil water content: measurements in coaxial transmission lines. Water Resour. Res. 16, 574–582.
Topp, G.C., Davis, J.L., Annan, A.P., 1982. Electromagnetic determination of soil water content using TDR, I, applications to wetting fronts and steep gradients. Soil Sci. Soc. Am. J. 46, 672–678.
Topp, G.C., Davis, J.L., 1985. Measurement of soil water content using time-domain reflectometry (TDR): a field evaluation. Soil Sci. Soc. Am. J. 49, 19–24.
Topp, G.C., Yanuka, M., Zebchuk, W.D., Zegelin, S., 1988. Determination of electrical conductivity using time domain reflectometry: soil and water experiments in coaxial lines. Water Resour. Res. 24, 945–952.
Vanclooster, M., Mallants, D., Diels, J., Feyen, J., 1993. Determining local-scale solute transport parameters using time domain reflectometry (TDR). J. Hydrol. 148, 93–107.
Vanclooster, M., Mallants, D., Vanderborght, J., Diels, J., van Orshoven, J., Feyen, J., 1995. Monitoring solute transport in a multi-layered sandy lysimeter using time domain reflectometry. Soil Sci. Soc. Am. J. 59, 337–344.
Vanderborght, J., Timmerman, A., Feyen, J., 2000. Solute transport for steady-state and transient flow in soils with and without macropores. Soil Sci. Soc. Am. J. 64, 1305–1317.
Vanderborght, J., Vanclooster, M., Timmerman, A., Seuntjens, P., Mallants, D., Kim, D.J., Jacques, D., Hubrechts, L., Gonzalez, C., Feyen, J., Diels, J., Deckers, J., 2001. Overview of inert tracer experiments in key Belgian soil types: relation between transport and soil morphological and hydraulic properties. Water Resour. Res. 37, 2873–2888.
Vogeler, I., Clothier, B.E., Green, S.R., Scotter, D.R., Tillman, R.W., 1996. Characterizing water and solute movement by time domain reflectometry and disk permeametry. Soil Sci. Soc. Am. J. 60, 5–12.
Vogeler, I., Clothier, B.E., Green, S.R., 1997. TDR estimation of electrolyte in the soil solution. Aust. J. Soil Res. 35, 515–526.
Wraith, J.M., Woodbury, B.L., Inskeep, W.P., Comfort, S.D., 1993. A simplified waveform analysis approach for monitoring solute transport using time-domain reflectometry. Soil Sci. Soc. Am. J. 57, 637–642. https://doi.org/10.2136/sssaj1993.03615995005700030002x.
Yanuka, M., Topp, G.C., Zegelin, S., Zebchuk, W.D., 1988. Multiple reflection and attenuation of time domain reflectometry pulses: theoretical consideration for application to soil and water. Water Resour. Res. 24, 945–952.
Yu, X., Yu, X. Time domain reflectometry tests of multi-layered soil. Proc. TDR 2006, Purdue University, West Lafayette, USA, Sept. 2006, Paper ID 3, 16p., http://engineering.purdue.edu/TDR/Papers.
Zhan, L.T., Mu, Q.Y., Chen, Y.M., Chen, R.P., 2013. Experimental study on applicability of using time-domain reflectometry to detect NAPLs contaminated sands. Sci. China Technol. Sci. 56, 1534–1543. https://doi.org/10.1007/s11431-013-5211-8.
Zhan, L., Mu, Q., Chen, Y. Detection of diesel-contaminated sands. Geo-Congres 2014, Technical Papers, GSP 234, ASCE, 2014.
Zhang, R.D., 2000. Generalized transfer function model for solute transport in heterogeneous soils. Soil Sci. Soc. Am. J. 64, 1595–1602.